International Journal of Refrigeration 131 (2021) 775–785

Contents lists available at ScienceDirect

International Journal of Refrigeration

journal homepage: www.elsevier.com/locate/ijrefrig

Refrigeration machine modeling for exergy-based performance and optimization potential evaluation of chillers in real field plants

Lorenz Brenner [a,b], Frank Tillenkamp [*,a], Christian Ghiaus [b]

[a] Zurich University of Applied Sciences (ZHAW), Institute of Energy Systems and Fluid-Engineering (IEFE), Technikumstrasse 9, Winterthur CH-8401, Switzerland
[b] Univ Lyon, CNRS, INSA-Lyon, Université Claude Bernard Lyon 1, CETHIL UMR5008, Villeurbanne, F-69621, France

ARTICLE INFO

Keywords:
Optimization potential assessment method
Modeling
Refrigeration plant
Refrigeration machine
Optimization potential index

Mots-clés:
Méthode d'évaluation du potentiel d'optimisation
Modélisation
Installation frigorifique
Machine frigorifique
Indice du potentiel d'optimisation

ABSTRACT

To investigate and optimize a refrigeration system, the behavior at various operating conditions must be known or determined. The performance and improvement possibilities may then be inferred from measurement data and compared with corresponding performance key figures. These values are typically referred to normal conditions and it is usually unknown which ones represent an adequate operation. However, it is relevant for refrigeration plant operators to have reference values for a large range of operation conditions as a baseline for determining the obtainable improvements. The present work proposes the application of steady-state models of refrigeration machines for increasing the range of applicability of the exergy-based optimization potential index method. Four different modeling approaches are evaluated and discussed: equation-fit, physical lumped parameter, refrigeration cycle and artificial neural network based models. The practical usage of the improved evaluation method is shown for the subsystem *refrigeration machine* on a real field installation as a case study. With the introduced additional limits for the optimization potential index, the interpretability of the results is increased. The distinction between adequate (technical requirements exceeded), acceptable (technical requirements fulfilled) and inadequate (potential for improvement) operation according to the state of the art in technology is straightforward, which is important in practice.

1. Introduction

A significant amount of the energy consumption in buildings is due to the heating, ventilation and air-conditioning (HVAC) systems. Depending on the climatic region, about 30 – 70% of the total energy consumption in air-conditioned buildings is due to systems for thermal comfort applications (Vakiloroaya et al., 2014). Thereby, more than 50% of this energy is consumed by refrigeration machines and plants (Wang et al., 2018). Consequently, the optimization of such systems may significantly reduce the energy consumption in air-conditioned buildings.

In order to investigate and optimize a refrigeration system, the behavior at various operating conditions must be known or determined. Exergy analysis is seen as an appropriate approach, as the electrical energy consumption of the refrigeration machines and auxiliary devices is the main expense in refrigeration plant operation. Electricity represents high quality energy which is degraded along the processes in the whole system. In refrigeration plants, the interest extends from the refrigeration machine itself to the neighboring hydraulic circuits, since a well-suited hydraulic integration of the chiller and an adequate operation of auxiliary devices is crucial in order to achieve a high efficiency of the plant. Furthermore, it is relevant for refrigeration plant operators to have reference values for determining the obtainable improvements. Interpretation of the results of the procedure should not require specialists to evaluate if there is a need to take action or not. For this reason, a practice-oriented evaluation method for refrigeration plants in air-conditioning applications based on exergy analysis and technical standards as baseline was introduced (Brenner et al., 2020a; 2020b). The method allows assessing the performance and the optimization potential with respect to the state of the art in technology and can be widely applicable in practice with most common measuring equipment of real field plants. In order to achieve this, the refrigeration plant is split into subsystems. This allows an individual assessment and leads to a reduction of the required measurement variables while still ensuring a sufficient level of detail. The optimization potential index (OPI) (Brenner et al., 2020b) relates the actual and the reference exergy input of a subsystem while the same output is achieved. The reference is considered according to the state of the art. Therefore, the key figure indicates how the real system would behave in comparison to a reference system

* Corresponding author. fax: +41 58 935 73 61.
E-mail address: frank.tillenkamp@zhaw.ch (F. Tillenkamp).

https://doi.org/10.1016/j.ijrefrig.2021.07.026
Received 8 February 2021; Received in revised form 19 May 2021; Accepted 21 July 2021
Available online 27 July 2021

Nomenclature

Abbreviations

AHU	air handling unit
ANN	artificial neural network
CL	subsystem cooling location
COP	coefficient of performance
CST	subsystem cold storage & transport
CV	coefficient of variation
DC	subsystem dry cooler
EF	equation fit
FC	subsystem free cooling
MAE	mean-absolute error
MSE	mean-squared error
HVAC	heating, ventilation and air-conditioning
NTU	number of transfer units
OPI	optimization potential index
PLP	physical lumped parameter
RC	refrigeration cycle
RM	subsystem refrigeration machine
RMSE	root-mean-squared error
R^2	coefficient of determination
VDMA	Verband Deutscher Maschinen und Anlagenbau

Variables

a	fitted parameter
A	heat exchanger surface area [m^2]
B	exergy [J]
c	specific heat capacity [J kg^{-1} K^{-1}]
h	specific enthalpy [J kg^{-1}]
$\dot{m}$	mass flow rate [kg s^{-1}]
n	number of data points
p	pressure [Pa]
Q	thermal energy [J]
$\dot{Q}$	heat flow rate (thermal power) [W]
s	specific entropy [J kg^{-1} K^{-1}]
T	temperature [K]
ΔT	temperature difference [K]
U	overall heat transfer coefficient [W m^{-2} K^{-1}]
W	work [J]
$\dot{W}$	power [W]
y	measured variable
$\bar{y}$	averaged measured variable
$\hat{y}$	modeled / predicted variable
ε	heat exchanger effectiveness [–]
η	efficiency [–]

Subscripts

act	actual
amb	ambient
c	condensation
C	condensator
CPR	compressor
e	evaporation
el	electrical
E	evaporator
HE	heat exchanger
in	input
isen	isentropic
meas	measured
mech	mechanical
out	output
r	refrigerant
RM	refrigeration machine
sc	subcooling
sh	superheating

Superscripts

acc	acceptable
adq	adequate
$*$	reference

in exactly the same situation and reveals the potential for improvement with respect to the technological baseline at a glance, regardless of the complexity of the system (see section 2 for details).

While for most subsystems enough data needed to derive the technological baseline from standards is available, this is generally not the case for refrigeration machines in real field plants. Specific baseline values for the electrical power consumption of the compressor are not available in technical standards because it depends on a variety of variables. Consequently, further research is required to specify additional reference values for the baseline in order to apply the OPI method in a wider range of operation conditions. Ideally, these values are determined with comprehensive and representative measurements. However, installing measurement equipment is always bound to investment costs and, therefore, most of the refrigeration machines are instrumented with the minimum number of sensors necessary for the operation. These measurements are rarely logged for monitoring purposes as the secondary side temperatures and cooling load is of main interest to the plant operators, e.g. for cost allocation of the connected consumers. Therefore, much attention was paid to refrigeration machine models as it is a suitable method to determine missing quantities or to predict the system behavior with currently available data.

Consequently, various studies handle the topic of refrigeration system analysis and optimization with the aid of numerical models of refrigeration machines or other field plant devices. Among others, Shan *et al.* proposed an improved chiller sequence control strategy for refrigeration plants with centrifugal chillers applying a multi-linear regression model (Shan et al., 2016). Typically, an optimal sequencing of the refrigeration machine operation can improve the plant efficiency and, therefore, reduce the electrical energy consumption. The authors showed an energy saving potential of 3% in comparison to the original control strategy. Wei *et al.* investigated a chiller plant with four refrigeration machines, four cooling towers and two cold water storage tanks (Wei et al., 2014). A data-driven approach was chosen to model the plant and, subsequently, to ameliorate the operating conditions. The model was applied with measurement data of two days and the authors demonstrated an energy consumption reduction of approximately 14%. Wang *et al.* handled the topic of chiller plant optimization to reduce the power consumption of the plant, by applying artificial neural network models to simulate the refrigeration machines and the cooling towers (Wang et al., 2018). Another study focused on the energy optimization of a multi-chiller plant with cooling towers in a multistory office building (Thangavelu et al., 2017). Energy models for the chillers, cooling towers and auxiliary devices were developed, in order to improve the energy utilization. For the optimization routine, the building load and ambient air conditions were used as inputs. The optimization delivered ideal on / off strategies of the equipment as well as chilled and cooling water conditions. By analysing three case studies, the authors identified an average energy saving of 20% for small chiller plants and up to 40% for moderate sized refrigeration systems.

The present work proposes the application of refrigeration machine models to introduce additional technical baseline values for the optimization potential index in the subsystem refrigeration machine. Four

different modeling approaches are investigated and discussed: equation-fit, physical lumped parameter, refrigeration cycle and artificial neural network based models. The parameters of all four models are identified experimentally by using commonly measured quantities in field plants as input variables in order to ensure the practical application of the evaluation method. Their usage and performance is evaluated with measurements from a real field installation. The best suiting model is then applied to calculate the optimization potential index. As a case study, the application of the assessment method for the subsystem refrigeration machine is exemplified with the experimental data obtained.

2. Assessment method

2.1. Definition of the optimization potential index (OPI)

The optimization potential index is given by Brenner et al. (2020b):

$$OPI = 1 - \frac{\frac{1}{24\,h}\int_{t=0\,h}^{24\,h} \dot{B}_{in}^{*}\,\mathrm{d}t}{\frac{1}{24\,h}\int_{t=0\,h}^{24\,h} \dot{B}_{in}\,\mathrm{d}t} = 1 - \frac{\sum_{t=0\,h}^{24\,h} B_{in}^{*}}{\sum_{t=0\,h}^{24\,h} B_{in}} \tag{1}$$

with B_{in} and B_{in}^{*} the mean values of the actual and reference (baseline) exergy input. The optimization potential index compares the exergy input of the actual system with a baseline according to the state of the art in technology. These reference values are derived from technical standards, as they are usually specified in tenders or contracts and should be fulfilled at the stage of commissioning. Also, these values represent an achievable technological baseline, which can depend on the requirements in different countries or regions. As the cooling load typically follows a daily dominant oscillation (i.e. negligible variation of energy and exergy stored during a day), the key figure is evaluated on a daily basis, e.g. for a daily check. The OPI can be interpreted as an averaged key figure, where the integrals in Eq. 1 are approximated by the sum of the means of measured values over the sampling interval. In the present evaluation, the field plant data available was recorded by the plant operator at an interval of 5 minutes which results in 288 summands for the daily assessment.

The interpretation of the results is straight-forward also for non-specialists, which is important in practice: If the actual effort is larger than the reference, an optimization potential is present which is indicated with an OPI greater than zero. Conversely, an OPI lower than zero indicates an adequate operation of the system where the technical requirements are exceeded. However, it is unknown which values close to OPI = 0 (technical requirements fulfilled) still represent a permissible operation, since the boundary between the two operating states is sharp (see Fig. 1a). By introducing an additional acceptable limit, OPI^{acc}, it can then be distinguished between adequate, acceptable and inadequate operation (see Fig. 1b), which yields a better interpretability of the results. This advanced assessment is introduced in the present study for the subsystem refrigeration machine.

2.2. Subsystem refrigeration machine

The optimization potential index for refrigeration machines is Brenner et al. (2020b):

$$OPI_{RM} = 1 - \frac{\sum_{t=0\,h}^{24\,h} B_{el,CPR}^{*}}{\sum_{t=0\,h}^{24\,h} B_{el,CPR}} = 1 - \frac{\sum_{t=0\,h}^{24\,h} W_{el,CPR}^{*}}{\sum_{t=0\,h}^{24\,h} W_{el,CPR}} \tag{2}$$

where $B_{el,CPR}$ and $B_{el,CPR}^{*}$ are the actual and reference (adequate) electrical exergy input of the compressor, respectively. Since electrical energy is by definition pure exergy, the key figure may be expressed in terms of the actual $W_{el,CPR}$ and reference electrical energy consumption of the compressor $W_{el,CPR}^{*}$. For the evaluation with three levels (red, yellow and green, Fig. 1b), it is proposed to define an additional acceptable boundary given by:

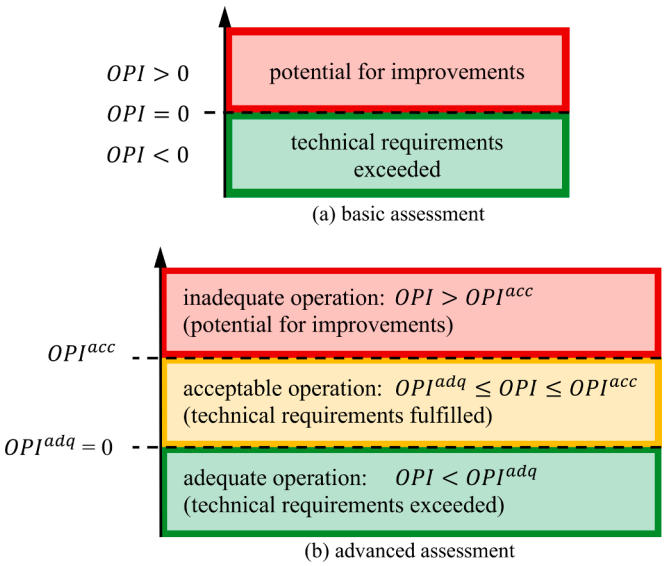

Fig. 1. Optimization potential index scale to determine the operation condition and improvement possibilities with respect to the technical baseline with (a) a basic and (b) an advanced assessment.

$$OPI_{RM}^{acc} = 1 - \frac{\sum_{t=0\,h}^{24\,h} W_{el,CPR}^{*}}{\sum_{t=0\,h}^{24\,h} W_{el,CPR}^{acc}} \tag{3}$$

where $W_{el,CPR}^{acc}$ is the acceptable electrical energy consumption of the compressor. As an approach, it is proposed to compute the reference (adequate) and acceptable compressor power consumption with a model of the refrigeration machine (see Section 4). The model should be as general as possible to assure a wide practical applicability of the presented method, independently of the system structure and even if no technical information of the refrigeration machine is available. Since the OPI represents a daily averaged key figure and the time response of the system components is significantly lower than 24 hours, a steady-state model is considered acceptable. Also, the model should have few parameters which can be experimentally identified with easily obtainable data with state-of-the-art measuring concepts in real field plants. Consequently, secondary side temperatures, the electrical power consumption of the compressor and the evaporator heat flow rate, which are commonly measured in field plants (see Section 3), are specified as input variables of the inverse model to identify the missing parameters (see Section 4). The reference electrical power consumption of the compressor $\dot{W}_{el,CPR}^{*}$ is then calculated by applying reference secondary side temperatures of the condenser ($T_{C,in}^{*}$ and $T_{C,out}^{*}$) together with the evaporator heat flow rate $\dot{Q}_{E}$, the cold water temperatures ($T_{E,in}$ and $T_{E,out}$) of the actual situation and the identified parameters as model inputs. In this paper it is proposed to define the reference secondary side inlet temperature of the condenser $T_{C,in}^{*}$ according to:

$$T_{C,in}^{*} = T_{C,in} - \left[\overline{T}_{C} - \overline{T}_{C}^{*}\right] \tag{4}$$

where $\overline{T}_{C}$ represents the logarithmic mean temperature at which the heat transfer at the condenser takes place in the actual situation. It is

defined as Brenner et al. (2020b):

$$\overline{T}_C = \frac{T_{C,out} - T_{C,in}}{\ln\left(\frac{T_{C,out}}{T_{C,in}}\right)} \tag{5}$$

with $T_{C,in}$ and $T_{C,out}$ the secondary side condenser inlet and outlet temperature, respectively. $\overline{T}_C^*$ in Eq. 4 represents the reference mean temperature (Brenner et al., 2020b):

$$\overline{T}_C^* = T_{amb} + \Delta T_{HE} + \frac{T_{C,out} - T_{C,in}}{2} \tag{6}$$

at which the heat transfer at the condenser takes place, if the hot side hydraulic circuit including the cooler is correctly operated and maintained according to the technical requirements. T_{amb} denotes the ambient air temperature and ΔT_{HE} the temperature difference in the cooler heat exchanger, i.e. cooling water outlet to ambient air inlet, according to technical standards. For the latter, a stricter value of 6 K is applied as reported in the technical standard VDMA 24247-8 (Mechanical Engineering Industry Association (VDMA), 2011) (see Table 1). Similarly, the reference secondary side outlet temperature of the condenser may be defined as:

$$T_{C,out}^* = T_{C,out} - \left[\frac{T_{C,out} - T_{C,in}}{\ln\left(\frac{T_{C,out}}{T_{C,in}}\right)} - \left(T_{amb} + \Delta T_{HE} + \frac{T_{C,out} - T_{C,in}}{2}\right)\right] \tag{7}$$

Therefore, these reference temperatures represent adequate values which should be achieved if the hot side hydraulic circuit, including the cooler, is correctly operated and maintained according to the technical standards. The reference condenser secondary side in- and outlet temperature is lower or higher than the measured temperature if the heat transfer takes place at a higher or lower temperature compared to the technical requirements, respectively. A lower cooling water temperature is favorable for the refrigeration machine operation.

The acceptable electrical power consumption of the compressor $\dot{W}_{el,CPR}^{acc}$ is determined analogously with the refrigeration machine model by applying acceptable secondary side temperatures of the condenser ($T_{C,in}^{acc}$ and $T_{C,out}^{acc}$). These temperatures are calculated similarly to Eq. 4 and 7 by applying the less stricter value for ΔT_{HE} according to Table 1.

3. Refrigeration plant structure

Fig. 2 shows schematically the typical refrigeration plant structure with cold water distribution and free cooling. Variables in italic represent commonly measured and monitored thermodynamic quantities of refrigeration machines in field plants and their corresponding measuring location. As a case study, an existing refrigeration plant installed in the city of Winterthur, Switzerland, is investigated in the present work. The field plant includes five refrigeration machines (see Fig. 2, subsystem RM) with 950 kW cooling power each and ammonia (R717) as refrigerant. Additionally, one free cooling heat exchanger (see Fig. 2, subsystem FC) is integrated to the system and the refrigeration machines as well as the distribution networks (see Fig. 2, subsystem CST) are located underground. The hydraulic circuit supplies seven different buildings with cold water, where the cooling locations (see Fig. 2, subsystem CL) represent air-handling units of ventilation systems in the different buildings with office space cooling as main application. Additionally, three rooftop coolers (see Fig. 2, subsystem DC), 12 circulating pumps and two cold water storage tanks are present in the system. The present work focuses on the subsystem refrigeration machine.

Table 1
Temperature differences in dry cooler heat exchangers according to VDMA 24247-8 (Mechanical Engineering Industry Association (VDMA) (2011)).

	Adequate	Acceptable
ΔT_{HE}	$\leq$ 6 K	$\leq$ 8 K

4. Investigated modeling approaches

Four models are investigated: two black-box models (equation-fit and artificial neural network based) and two gray-box models (physical lumped parameter and refrigeration cycle based). All models use measured secondary side quantities as inputs ($T_{E,in}$, $T_{E,out}$, $T_{C,in}$, $T_{C,out}$, $\dot{Q}_E$) and a procedure for finding the values of the parameters which minimizes the difference between the measured output ($\dot{W}_{el,CPR}$) and the output of the model.

4.1. Equation-fit based model

Equation-fit based (EF) models are purely empirical and do not aim to fully characterize each component in the refrigeration machine, but to predict certain key performance parameters such as the coefficient of performance (COP), the cooling load or the compressor power consumption.

The Comstock model has been chosen as equation-fit based model, as it uses commonly measured quantities in field plants as input variables to determine the compressor electrical power consumption. It is a second-order polynomial fitting model with 7 fitting parameters a_i to determine the compressor electrical power consumption (Wang, 2017):

$$\dot{W}_{el,CPR} = a_1 + a_2 T_{E,in} + a_3 T_{C,in} + a_4 \dot{Q}_E + a_5 T_{E,in}\dot{Q}_E + a_6 T_{C,in}\dot{Q}_E + a_7 \dot{Q}_E^2 \tag{8}$$

with $T_{E,in}$ the evaporator secondary side inlet temperature, $T_{C,in}$ the condenser secondary side inlet temperature and $\dot{Q}_E$ the evaporator heat flow rate as input parameters. The coefficients a_i reveal no physical characteristic and are determined from measurement data with the *lsqcurvefit* curve-fitting algorithm pre-implemented in MATLAB (MAT, 2018).

4.2. Physical lumped parameter model

Physical lumped parameter (PLP) models are grey-box models and make use of thermodynamic or heat transfer relations to build the model structure based on semi-empirical equations and require experimental data to obtain missing parameters. They generally have a similar form as the equation-fit based models.

In the present work, the Folicao model is applied as physical lumped parameter model. It uses commonly measured quantities in field plants as input variables like the Comstock model. It is a three-parameter model which has the following form Foliaco et al. (2020):

$$\dot{W}_{el,CPR} - \left(\frac{T_{C,in} - T_{E,out}}{T_{E,out}}\right)\dot{Q}_E = a_1 T_{C,in} + a_2\left(\frac{T_{C,in} - T_{E,out}}{T_{E,out}}\right) + a_3\left(\frac{\dot{Q}_E^2 + \dot{Q}_E \dot{W}_{el,CPR}}{T_{E,out}}\right) \tag{9}$$

with $T_{E,out}$ the evaporator secondary side outlet temperature, $T_{C,in}$ the condenser secondary side inlet temperature and $\dot{Q}_E$ the evaporator heat flow rate as inputs parameters. The fitting parameters are determined with the regression routine *regress* pre-implemented in MATLAB (MAT, 2018), where a_1 denotes the entropy generation in the refrigeration cycle, a_2 the heat losses or gains from the refrigeration machine and a_3 the total heat exchanger thermal resistance.

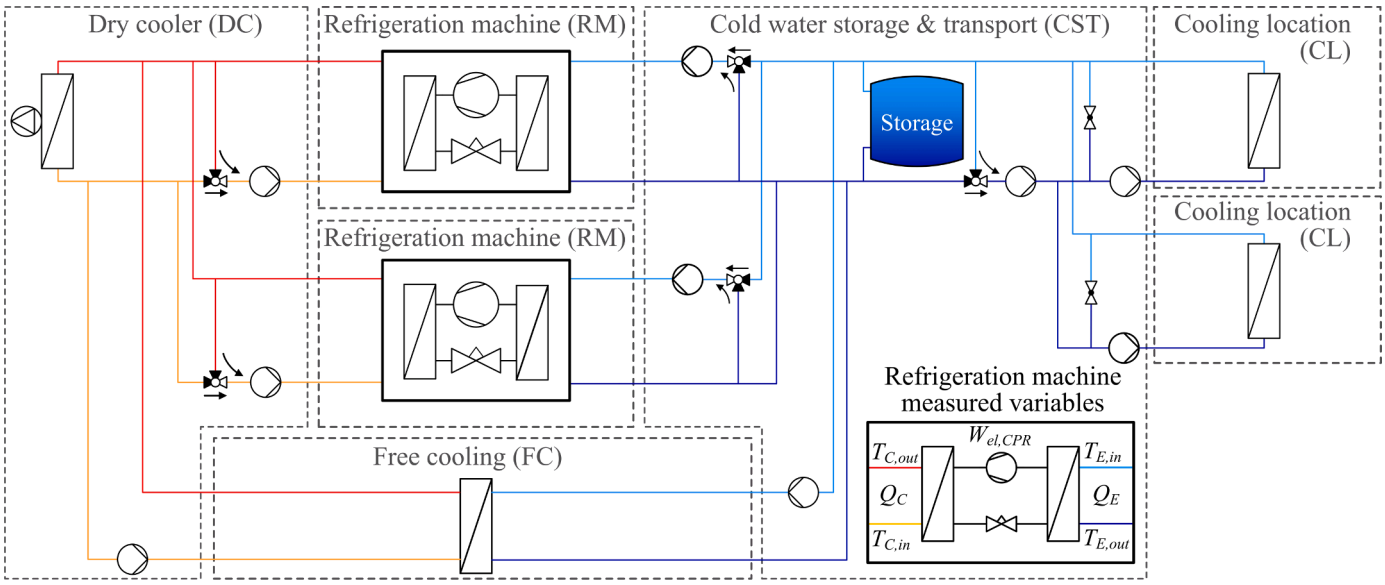

Fig. 2. Simplified piping & instrumentation diagram of a typical refrigeration plant with cold water distribution and a free cooling module, i.e. heat exchanger. Commonly measured and monitored variables of refrigeration machines in field plants are shown in italic.

4.3. Refrigeration cycle based model

Refrigeration cycle based (RC) models, also denoted physical component based models, aim to evaluate and predict the evolution of the refrigerant and its thermodynamic states during the passage through each refrigeration machine component, where it is exposed to compression, expansion as well as heat gains and losses. Usually, the nodal approach is applied, where the main components (compressor, evaporator, condenser and expansion valve) are modeled separately and then connected to each other in order to simulate the whole refrigeration cycle.

A simplified refrigeration cycle based model is applied in the present work which represents a gray-box fitting model. It considers the four main refrigeration machine components (evaporator, compressor, condenser and expansion valve) in terms of thermodynamic and heat transfer relations. Fig. 3 shows a schematic of the considered refrigeration cycle as well as the corresponding log(p)-h-diagram with the different refrigerant states. The thermo-physical properties of the refrigerant are computed with the tool REFPROP (Reference Fluid Thermodynamic and Transport Properties Database) (Bell et al., 2013). The model uses secondary side temperatures as well as the evaporator heat flow rate as input variables and incorporates 6 physical parameters (see Table 2 for details), which are identified from measurement data. To reduce the number of unknown parameters, the following assumptions apply to the model:

- steady-state operation,
- negligible heat exchange with the environment,
- negligible pressure losses,
- isenthalpic expansion.

With the given simplifications, the chosen refrigeration cycle may differ from the real system structure and, consequently, the identified parameters may not represent the actual physical conditions. However, the model is still able to predict the compressor electrical power with a reduced amount of required data. Therefore, to the best of the authors knowledge, these simplifications are reasonable and ensure a broad applicability of the presented method.

The evaporator and condenser are modeled with the NTU-ε effectiveness method and are considered as heat exchangers with phase change on the primary side. This represents a special case, where the heat capacity rates of the condensing vapor or evaporating liquid tends towards infinity (nearly isothermal processes). The evaporator effectiveness ε_E is then given by Incropera et al. (2014); Jin and Spitler (2002):

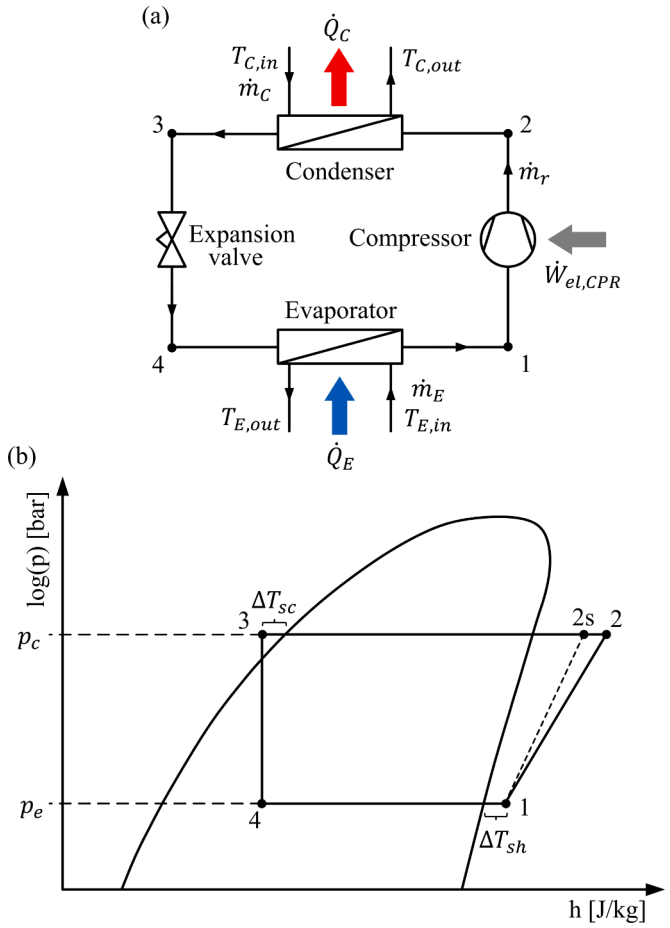

Fig. 3. Simplified schematic of (a) the considered refrigeration cycle and (b) the corresponding log(p)-h-diagram with the different refrigerant states 1 to 4 and 2s.

Table 2
Inputs, outputs and parameters of the RC based model.

Type	Variables	
input	$T_{E,in}$	evaporator secondary side inlet temperature
	$T_{E,out}$	evaporator secondary side outlet temperature
	$T_{C,in}$	condenser secondary side inlet temperature
	$T_{C,out}$	condenser secondary side outlet temperature
	$\dot{Q}_E$	evaporator heat flow rate
output	$\dot{W}_{el,CPR}$	compressor electrical power
parameter	η_{isen}	compressor isentropic efficiency
	$\eta_{el,mech}$	compressor electro-mechanical efficiency
	ΔT_{sh}	superheating temperature difference
	ΔT_{sc}	subcooling temperature difference
	$(UA)_E$	evaporator surface dependent overall heat transfer coefficient
	$(UA)_C$	condenser surface dependent overall heat transfer coefficient

$$\varepsilon_E = 1 - e^{-NTU_E} \tag{10}$$

where NTU_E denotes the dimensionless parameter *number of transfer units* of the evaporator, which is defined as Incropera et al. (2014):

$$NTU_E = \frac{(UA)_E}{c_{p,E}\dot{m}_E} \tag{11}$$

with $(UA)_E$ the overall heat transfer coefficient times the heat transfer area of the evaporator as well as $c_{p,E}$ and $\dot{m}_E$ the specific heat capacity and the mass flow rate of the secondary side chilled water, respectively. As the heat capacity and mass flow rate of the secondary side are unknown, their product can be determined with an energy balance over the evaporator. The evaporation temperature of the refrigerant is then given by Incropera et al. (2014); Jin and Spitler (2002):

$$T_e = T_{E,in} - \frac{\Delta T_E}{\varepsilon_E} \tag{12}$$

where $T_{E,in}$ denotes the evaporator secondary side inlet temperature and ΔT_E the secondary side inlet to outlet temperature difference. Analogously, Eq. 10 to 12 apply also for the condenser by utilizing the corresponding quantities. With the chosen NTU-ε effectiveness approach, the superheating and subcooling effects in the heat exchangers are not explicitely treated. However, the error is assumed negligible, as it is presumably compensated with the *UA* parameter when calibrating the model. With the evaporation and condensation temperature, the low and high pressure level, p_e and p_c (see Fig. 3b), can be determined. The refrigerant temperature T_1 at state 1 after the evaporator (see Fig. 3) is:

$$T_1 = T_e + \Delta T_{sh} \tag{13}$$

where ΔT_{sh} represents the superheating temperature difference. Similarly, the refrigerant temperature T_3 at state 3 after the condenser (see Fig. 3) is:

$$T_3 = T_c - \Delta T_{sc} \tag{14}$$

where ΔT_{sc} is the subcooling temperature difference. Together with the found pressures, the specific enthalpies and entropies (h_1, h_3, s_1, s_3) of the refrigerant can be identified at state 1 and 3. By assuming an isenthalpic expansion process, the specific enthalpy h_4 at state 4 after the expansion valve (see Fig. 3) is equivalent to the specific enthalpy h_3 at state 3. With an energy balance, the evaporator heat flow rate $\dot{Q}_E$ is given by Dinçer and Kanoğlu (2010); Moran et al. (2010):

$$\dot{Q}_E = \dot{m}_r(h_1 - h_4) \tag{15}$$

from which the refrigerant mass flow rate $\dot{m}_r$ can be determined. The actual compressor input $\dot{W}_{CPR,act}$ is Dinçer and Kanoğlu (2010); Moran et al. (2010):

$$\dot{W}_{CPR,act} = \dot{m}_r(h_2 - h_1) \tag{16}$$

where the enthalpy h_2 at state 2 after the compressor must be known (see Fig. 3). The compressor isentropic efficiency η_{isen} is given by Dinçer and Kanoğlu (2010); Moran et al. (2010):

$$\eta_{isen} = \frac{\dot{W}_{CPR,isen}}{\dot{W}_{CPR,act}} = \frac{\dot{m}_r(h_{2s} - h_1)}{\dot{m}_r(h_2 - h_1)} = \frac{h_{2s} - h_1}{h_2 - h_1} \tag{17}$$

which relates the isentropic compressor input $\dot{W}_{CPR,isen}$ with the actual compressor power $\dot{W}_{CPR,act}$, where h_{2s} represents the specific enthalpy resulting from an isentropic (i.e. reversible) compression (see Fig. 3). By rearranging Eq. 17, h_2 can be identified, and finally, the compressor electrical power determined: (Ozgur et al., 2014):

$$\dot{W}_{el,CPR} = \frac{\dot{W}_{CPR,act}}{\eta_{el,mech}} \tag{18}$$

where $\eta_{el,mech}$ represents the compressor electro-mechanical efficiency to account for mechanical as well as electrical losses. The condenser heat flow rate $\dot{Q}_C$ is given with an overall energy balance over the refrigeration cycle (Dinçer and Kanoğlu, 2010):

$$\dot{Q}_C = \dot{Q}_E + \dot{W}_{CPR,act} \tag{19}$$

The condenser heat flow rate is unknown in the beginning, guessed for the initial iteration and then iteratively computed with the described procedure, until the relative error is lower than 0.1%. A cost function, chosen to be the root-mean-squared error (RMSE, see subsection 4.5) between the modeled and measured compressor electrical power, is minimized to identify the models parameters (see Table 2). These are initially determined with a batch gradient-descent routine (Ruder, 2017) and then iteratively optimized with the pre-implemented minimization algorithm *fmincon* in MATLAB (MAT, 2018). All parameters reveal a physical characteristic and defining them as constants is physically not correct (except in steady-state). However, to the best of the authors knowledge, this simplification is reasonable with the goal of having a widely applicable model which can be employed independently of the compressor and heat exchanger design, even if no technical details of the refrigeration machine are available.

4.4. Artifical neural network model

Artificial neural networks (ANN) are data-driven black-box models with no physical meaning which are inspired by the biological nervous system. The ANNs comprise a set of simple elements in parallel, the so called neurons, which have a weighted connection between each other in different layers. This results in a construct of multiple mathematical functions, which relates a set of inputs to certain outputs (Kalogirou, 2000). Depending on the application, ANNs can be composed of any number of neurons and arranged in different structures.

In the present work, a feed-forward ANN model is applied with one input layer, one ouput layer and one hidden layer (see Fig. 4), which has been determined by trial and error. Like the refrigeration cycle based model, the ANN has 5 input parameters (secondary side temperatures as well as evaporator heat flow rate) and one output parameter, the compressor electrical power $\dot{W}_{el,CPR}$. A tan-sigmoid and a linear activation function is used for the hidden and output layer, respectively. The hidden layer consists of 25 neurons (with bias). The amount of neurons was identified by iteratively increasing the number until the performance function, chosen to be the mean-squared error (MSE), was minimized. The latter is defined as Datta et al. (2019):

$$MSE = \frac{1}{n}\sum_{i=1}^{n}\left(\hat{y}_i - y_i\right)^2 \tag{20}$$

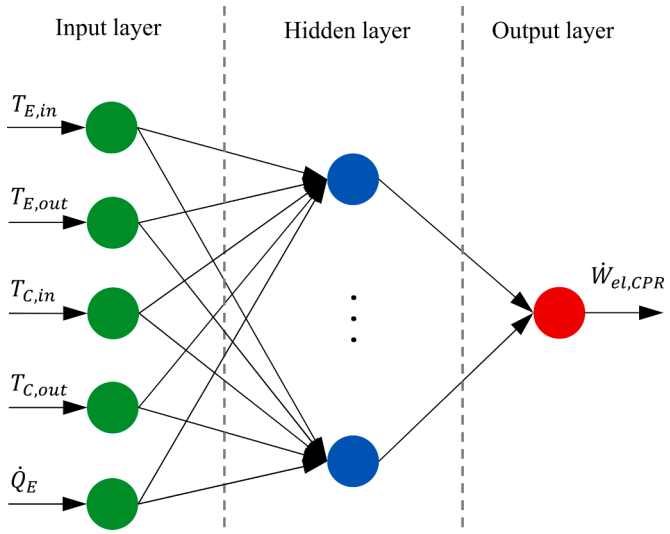

Fig. 4. Topology of the applied feed-forward neural network with the corresponding input and output variables.

where y_i represents the measured value, $\hat{y}_i$ the predicted value and n the number of data points. The number of neurons is substantially lower than the number of training data points, which reduces the risk of overfitting. The ANN is designed, set-up and trained with the *Deep Learning Toolbox* (functions *feedforwardnet* and *train*) pre-implemented in MATLAB (MAT, 2018). One of the most popular learning method is the back-propagation, which is a gradient-descent based procedure (Kalogirou, 2000). In the present work, the Levenberg-Marquardt back-propagation algorithm is applied for training (Hagan and Menhaj, 1994), which is particularly useful for moderate-sized ANNs with the MSE as performance function (Hagan et al., 2014).

4.5. Model performance metrics

Many different performance indicators exist, which can be applied to evaluate the model accuracy. In the present work, the following indicators are applied, where y_i represents the measured value, $\hat{y}_i$ the predicted value and n the number of data points. One of the most applied index is the root-mean-squared error (RMSE) (Şahin, 2011):

$$RMSE = \sqrt{\frac{1}{n}\sum_{i=1}^{n}\left(\hat{y}_i - y_i\right)^2} \tag{21}$$

The second index is the mean-absolute error (MAE) which has an increased interpretability compared to the RMSE, which is Wang (2017):

$$MAE = \frac{1}{n}\sum_{i=1}^{n}\left|\hat{y}_i - y_i\right| \tag{22}$$

The coefficient of variation of the root-mean-squared error (CV or CV-RMSE), also denoted relative root-mean-squared error (R-RMSE), indicates if the model has a satisfactory prediction ability, where a small value indicates a high predictive accuracy. The indicator is defined with Wang (2017):

$$CV = \frac{RMSE}{\bar{y}_i}\cdot 100\% \tag{23}$$

where $\bar{y}_i$ is the average of the measured values. Additionally, the coefficient of determination (R^2) is applied, which is given by Şahin (2011):

$$R^2 = 1 - \frac{\sum_{i=1}^{n}\left(y_i - \hat{y}_i\right)^2}{\sum_{i=1}^{n}\left(y_i - \bar{y}_i\right)^2} \tag{24}$$

This indicator relates the sum of the squared residuals (deviation from the predicted and measured value) with the total sum of squares. The closer the value of R^2 is to 1, the more accurate are the modeled values.

5. Results and discussion

5.1. Refrigeration machine model comparison

Fig. 5 depicts the modeled compressor electrical power consumption of each modeling approach (y-axis) in function of the measured compressor electrical power consumption (x-axis) with a ±10% error band. Table 3 lists the values of the different performance indicators for each model with respect to the training / validation and testing data. For the former, measurement data of refrigeration machine 1 (RM1, 12,430 data points) installed in the investigated field plant (see Fig. 2) are applied, where a share of 60 and 40% is used for training and validation, respectively. Measurement data of refrigeration machine 2 (RM2, 12,250 data points) is applied as testing data set. The number of data points represents all the measuring points in the investigated time period (sampling time from April to December) according to the received data of the plant operator, where the corresponding refrigeration machine was running, i.e. electrical power consumption of the compressor was larger zero. The measured compressor electrical power ranges from 1 to 195 kW and from 1 to 184 kW in the training / validation and testing data set, respectively, where a large range of different operating conditions are present (part load as well as full load).

To start with, the equation-fit based (EF) model reveals with the training / validation data a root-mean-squared (RMSE) and mean-absolute error (MAE) value of 3.23 and 2.36 kW (see Table 3), respectively, where the values are reasonable with the given range of the compressor electrical power. Similar values are achieved with the testing data set, which has not been used for training. The physical lumped parameter (PLP) model reveals a similar performance as the equation-fit based model, where the RMSE and MAE values range depending on the data set from 3.15 to 3.2 kW and 2.44 to 2.55 kW, respectively (see Table 3). Furthermore, the refrigeration cycle (RC) based model performs worst among the investigated modeling approaches. This outcome is most likely due to the constant model parameters, which would vary in reality. A large range of different operating states is present in the experimental data of the field plant, which complicates the identification of valid parameters for all load conditions. The predicted power consumption by the artificial neural network (ANN) model shows qualitatively a good agreement with measurements when using both data sets (see Fig. 5d). Since ANN models interpolate well, this outcome is most likely due the large training domain, where all kind of part and full load conditions are covered. Also, all refrigeration machines in the field plant are of the same type and size, whereby most likely all of them reveal a similar operating behavior. The adequate performance is also demonstrated with R^2 values close to 1 and CV values below 3%, where only approximately 10% of the simulated values are outside of the ±10% error band.

When comparing the different models, all approaches perform only slightly worse with the testing data set, where the equation-fit based and physical lumped parameter model reveal a similar performance. The reason is probably the large training domain, where all kind of operation conditions are covered and that the refrigeration machines are identical. The refrigeration cycle based model underpredicts the compressor power significantly in part load conditions (see Fig. 5c), which contributes to the highest key figure values compared to the other

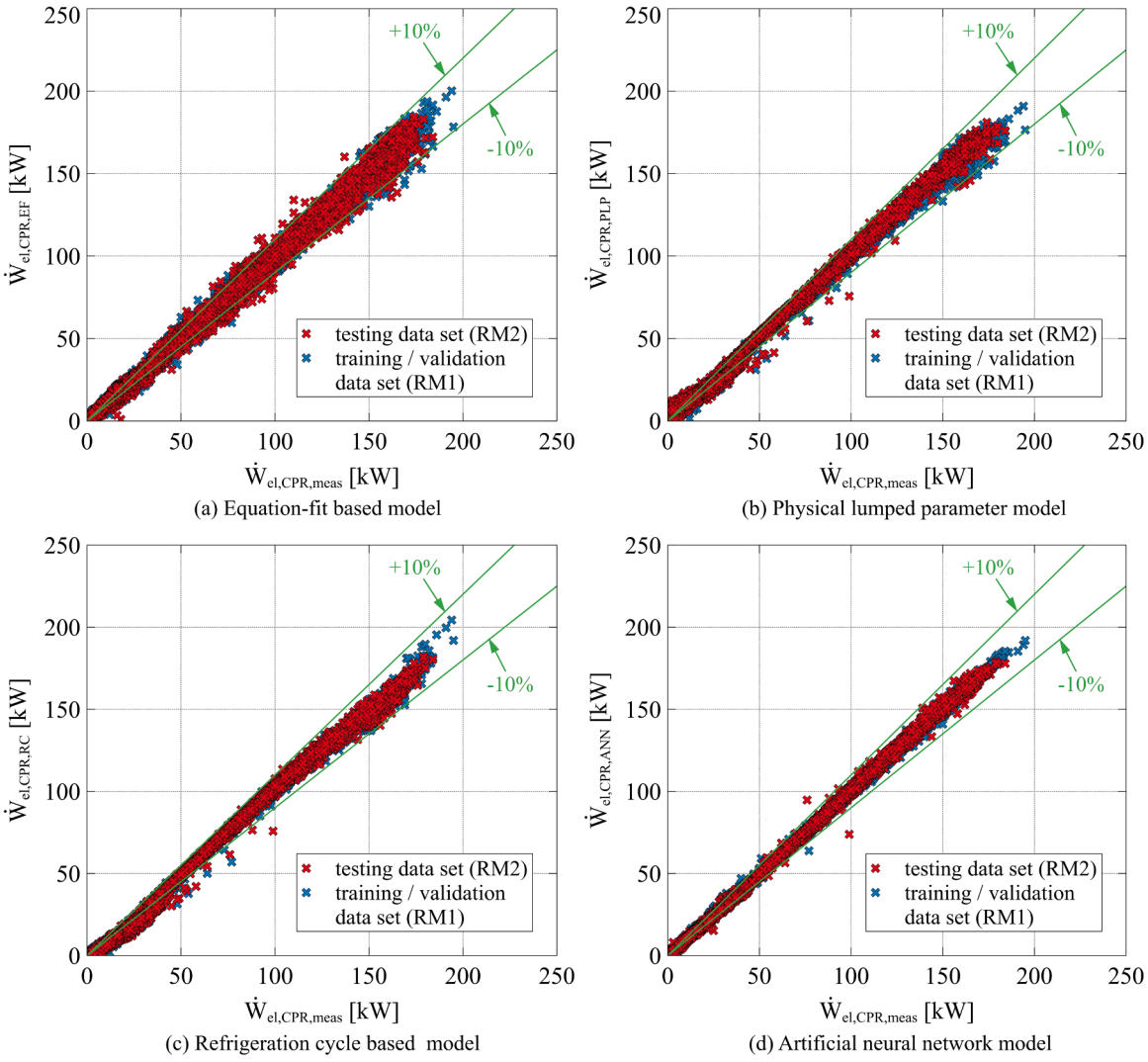

Fig. 5. Comparison of the measured and modeled compressor electrical power consumption of the refrigeration machines in the field plant: (a) equation-fit based model, (b) physical lumped parameter model, (c) refrigeration cycle based model and (d) artifical neural network model.

Table 3
List of the RMSE, MAE, R^2 and CV values for each modeling approach with respect to the training / validation (RM1) and testing (RM2) data of the refrigeration machines in the field plant.

Performance indicator	Equation-fit based model		Phyiscal lumped parameter model	
	RM1	RM2	RM1	RM2
root-mean-squared error (RMSE) [kW]	3.23	3.26	3.15	3.20
mean-absolute error (MAE) [kW]	2.36	2.34	2.44	2.55
coefficient of determination (R^2) [–]	0.995	0.994	0.995	0.995
coefficient of variation (CV) [%]	6.36	6.34	6.20	6.22
	Refrigeration cycle based model		Artificial neural network model	
	RM1	RM2	RM1	RM2
root-mean-squared error (RMSE) [kW]	4.02	4.24	1.12	1.45
mean-absolute error (MAE) [kW]	3.16	3.40	0.80	1.07
coefficient of determination (R^2) [–]	0.992	0.991	0.999	0.999
coefficient of variation (CV) [%]	7.91	8.25	2.21	2.82

investigated models. All performance indicators reveal acceptable values except the coefficient of variation, where only the ANN model reaches values lower than 5%, which is adequate for a practical application of the model (Hydeman et al., 2002; Wang, 2017). Consequently, the ANN model is applied for the optimization potential index. By using reference and acceptable temperatures on the condenser secondary side according to technical standards, the reference and acceptable compressor power consumption can be simulated (see subsection 2.2).

5.2. *Refrigeration machine performance analysis*

By applying the method described in subsection 2.2, together with the acquired measurement data from the field plant and the ANN model, the corresponding OPI of each refrigeration machine is determined. The analysis should further demonstrate the usage of the evaluation approach and reveal the performance as well as eventual optimization potentials of the refrigeration machines. According to the available experimental data, refrigeration machine operation occurred mainly from begin of April to end of October. Fig. 6 shows the daily optimization potential index (OPI, y-axis) of the subsystem RM (see Fig. 2) in the field plant under investigation in function of the date (x-axis).

The daily OPI is indicated with data points, where the 14-days moving average is represented by a solid line to evaluate the tendency over time. The green, yellow and red zone depicts the adequate, acceptable and inadequate operation condition, respectively. The adequate boundary is always at OPI = 0 according to the key figure definition (comparison of the reference with the actual effort), while the acceptable limit may fluctuate due to dependencies of various parameters at the different operating points (comparison of the reference with

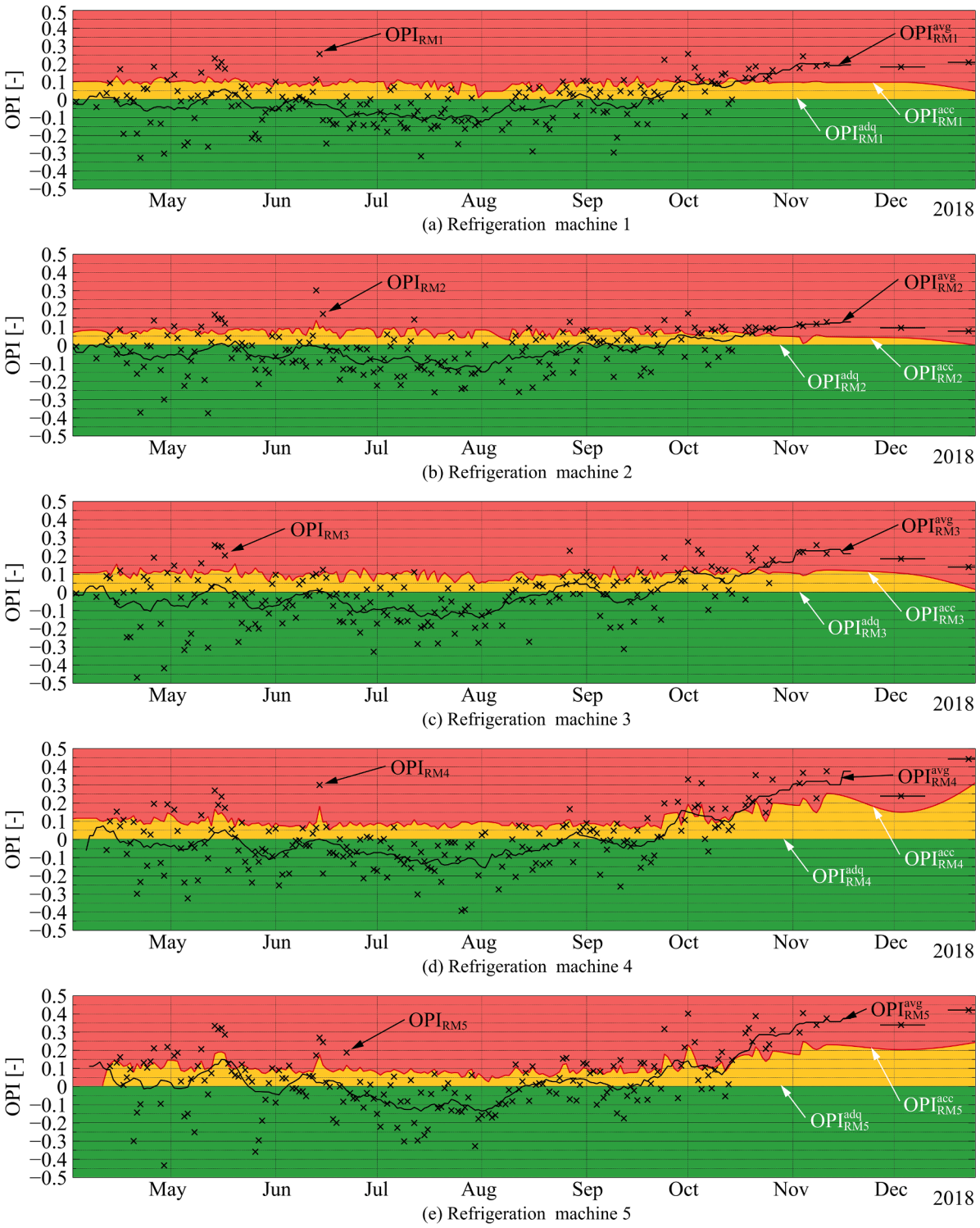

Fig. 6. Optimization potential index OPI_{RM} of (a) refrigeration machine 1 to (e) refrigeration machine 5 with adequate (green), acceptable (yellow) and inadequate (red) operation range. The data points (black crosses) represent the daily OPI values and the black solid line indicates the 14-days moving average of the OPI. (For interpretation of the references to colour in this figure legend, the reader is referred to the web version of this article.)

the acceptable effort). Additionally, missing data points for the acceptable limit were determined by interpolation, since not all refrigeration machines were running every day.

The optimization potential index of the five different refrigeration machines lies in the range from –0.47 to 0.44 (see Fig. 6a to 6e), whereas the maximum difference in OPI of 0.43 between two chillers (RM4 and RM5) is reached on June 15th. Refrigeration machine 2 yields the lowest average optimization potential index OPI_{RM2} of –0.03 (see Fig. 6b), while the key figure scatters the least among all refrigeration machines. The system operates approximately 80% of the time below the acceptable boundary OPI^{acc}_{RM2}, where 60% and 20% of the time an adequate and acceptable operation of the subsystem is achieved, respectively. Conversely, refrigeration machine 5 yields the highest average key figure among all refrigeration machines of 0.02 (see Fig. 6e). In 44% and

29% of the time in the investigated period the technical requirements are exceeded and fulfilled, respectively. The refrigeration machine was commissioned on April 13th, and therefore, no key figures are present before that day. The late commissioning of the machine may also be the reason for the differentiated behavior compared to the other devices. Overall, OPI_{RM1} to OPI_{RM5} are at least 73% of the time in adequate and acceptable operation range. This indicates a reasonable performance of all refrigeration machines and their hydraulic integration, where mostly little to no optimization potential compared to the state of the art in technology is present.

Interestingly, by examining the moving average OPI_{RM}^{avg} of all refrigeration machines, they reveal a similar operation. Analogue tendencies of an increasing and decreasing OPI are observed. Presumably, this is due to the same type and size of all installed refrigeration machines, e.g. redundancy purposes, where each of them are operated comparably. Moreover, it is revealed that during the warmer months over the year, i.e. June to end of August, all refrigeration machines exceed and fulfill the technical requirements. This leads to the assumption that the chillers are working near to or at the design point and that the hot side hydraulic circuit is properly operating. The refrigeration machines reveal an increase of the OPI in the transition period, i.e. April, May and September, where mostly an acceptable operation is present. A further noticeable increase in OPI is observed in the colder months October to December, where generally an inadequate operation is present. However, the systems are operating infrequent in this time period, since there is a significant lower need for cooling, and single outliers should not be overly considered. Most likely, the refrigeration machines are not operating at the design point in the mentioned time period or the temperature level on the hot side hydraulic circuit is not ideal, where the latter can result in an increased electrical power consumption of the compressors. According to literature, lowering the condensing temperature (which is highly influenced by the hot side hydraulic circuit) by 1 K, can reduce the energy consumption of the refrigeration plant by up to 2.5% as a rule of thumb (Brunner et al., 2019). The increased OPI values in the colder months can also be an indicator to make use of free cooling, which is typically active in this period. Furthermore, errors resulting from the ANN model are possible, since errors in part load conditions may have an increased effect. However, to the best of the authors knowledge, these errors are assumed negligible according to the model performance (see subsection 5.1). To finally determine the issues in the subsystem RM in the mentioned time period a detailed analysis would be necessary, assuming the needed experimental data is available.

6. Conclusions and outlook

The present work demonstrates successfully the use of refrigeration machine models for the integration in the optimization potential index. The practical application is shown by applying the method to a real field installation as a case study. With the introduced additional limits, a more detailed assessment with the evaluation method is achieved and the interpretability of the results is increased. The distinction between adequate (technical requirements exceeded), acceptable (technical requirements fulfilled) and inadequate (potential for improvement) operation according to the state of the art in technology is straightforward and the results are simple to interpret, which is important in practice. In that way, refrigeration plant operators can track the refrigeration machine performance on a daily basis and a simple colored indicator could be realized for the implementation in monitoring systems. To the best of the authors knowledge, an analysis with the described method (revealing possible optimization potentials in a first step), together with a detailed analysis (identify the malfunction in detail in a second step and evaluate if adjustments are worthwhile also from an economic point of view), delivers a target-oriented procedure to analyze the refrigeration plant behavior and to optimize the system efficiency.

Moreover, all examined models reveal an acceptable performance, where the mean-absolute error ranges from 0.8 to 3.4 kW. This values are considered reasonable, with the given range of the measured compressor electrical power consumption. However, only the ANN model reaches coefficient of variation values lower than 5%, which represents an adequate value for a practical application. Consequently, this modeling approach is applied for the determination of the optimization potential index. The investigated refrigeration machines of the field plant generally fulfill or exceed the technical requirements. Refrigeration machine 2 performs best with an average optimization potential index of –0.03. Refrigeration machine 5 performs worst, while being 73% of the time in adequate or acceptable operation. Moreover, all refrigeration machines show potential for improvement in the colder months. This can be an indicator to make use of free cooling, which is typically active in this time period.

Future work could cover the investigation of additional machine learning algorithms or models for the other subsystems in the refrigeration plant. This can increase the level of detail of the analysis and may help to assess refrigeration plants with a reduced amount of installed measuring equipment. In this context, further measurement data should be collected from other real refrigeration plants, preferably with different cooling capacities and sizes. The practical application of the evaluation method could then be elaborated in detail and interrelations between various field plants might be identified.

Declaration of Competing Interest

The authors declare that they have no known competing financial interests or personal relationships that could have appeared to influence the work reported in this paper.

Acknowledgements

This study was partially funded by the Swiss Federal Office of Energy (SFOE).

References

Bell, I., Huber, M. L., McLinden, M. O., Lemmon, E. W., 2013. NIST Reference Fluid Thermodynamic and Transport Properties Database (REFPROP) Version 9 - SRD 23, National Institute of Standards and Technology. 10.18434/T4JS3C.

Brenner, L., Tillenkamp, F., Ghiaus, C., 2020. Exergy performance and optimization potential of refrigeration plants in free cooling operation. Energy 209, 118464. https://doi.org/10.1016/j.energy.2020.118464.

Brenner, L., Tillenkamp, F., Krütli, M., Ghiaus, C., 2020. Optimization potential index (OPI): an evaluation method for performance assessment and optimization potential of chillers in HVAC plants. Appl Energy 259. https://doi.org/10.1016/j.apenergy.2019.114111.

Brunner, A., Kriegers, M., Prochaska, V., Tillenkamp, F., 2019. Klimakälte heute - Kluge Lösungen für ein angenehmes Raumklima. Faktor Verlag, Zürich.

Şahin, A.S., 2011. Performance analysis of single-stage refrigeration system with internal heat exchanger using neural network and neuro-fuzzy. Renew Energy 36 (10), 2747–2752. https://doi.org/10.1016/j.renene.2011.03.009.

Datta, S.P., Das, P.K., Mukhopadhyay, S., 2019. An optimized ANN for the performance prediction of an automotive air conditioning system. Science and Technology for the Built Environment 25 (3), 282–296. https://doi.org/10.1080/23744731.2018.1526014.

Dinçer, İ., Kanoğlu, M., 2010. Refrigeration systems and applications. Wiley, Chichester. https://doi.org/10.1002/9780470661093.

Foliaco, B., Bula, A., Coombes, P., 2020. Improving the Gordon-Ng model and analyzing thermodynamic parameters to evaluate performance in a water-cooled centrifugal chiller. Energies 13 (9), 2135. https://doi.org/10.3390/en13092135.

Hagan, M.T., Demuth, H.B., Beale, M.H., De Jesus, O., 2014. Neural network design. Oklahoma State University, Stillwater, OK.

Hagan, M.T., Menhaj, M.B., 1994. Training feedforward networks with the marquardt algorithm. IEEE Trans. Neural Networks 5 (6), 989–993. https://doi.org/10.1109/72.329697.

Hydeman, M.M., Sreedharan, P., Webb, N., Blanc, S., 2002. Development and testing of a reformulated regression-based electric chiller model. ASHRAE Transactions 180 (2).

Incropera, F.P., Dewitt, D.P., Bergman, T.L., Lavine, A.S., 2014. Principles of heat and mass transfer. John Wiley & Sons, Hoboken, NJ.

Jin, H., Spitler, J., 2002. A parameter estimation based model of water-to-water heat pumps for use in energy calculations programs. ASHRAE Transactions 108 (1), 3–17.

MATLAB version 9.4.0.813654 (R2018a), 2018. The Mathworks Inc.Natick, Massachusetts.
Kalogirou, S.A., 2000. Applications of artificial neural-networks for energy systems. Appl Energy 67 (1–2), 17–35. https://doi.org/10.1016/S0306-2619(00)00005-2.
Mechanical Engineering Industry Association (VDMA), 2011. Energieeffizienz von Klimakälteanlagen. Teil 8: Komponenten - Wärmeübertrager (VDMA 24247-8).
Moran, M.J., Shapiro, H.N., Boettner, D.D., Bailey, M.B., 2010. Fundamentals of engineering thermodynamics: SI version. Wiley, New York.
Ozgur, A.E., Kabul, A., Kizilkan, O., 2014. Exergy analysis of refrigeration systems using an alternative refrigerant (HFO-1234yf) to R-134a. International Journal of Low-Carbon Technologies 9 (1), 56–62. https://doi.org/10.1093/ijlct/cts054.
Ruder, S., 2017. An overview of gradient descent optimization algorithms. 1609.04747.
Shan, K., Wang, S., Gao, D.C., Xiao, F., 2016. Development and validation of an effective and robust chiller sequence control strategy using data-driven models. Autom. Constr. 65, 78–85. https://doi.org/10.1016/j.autcon.2016.01.005.
Thangavelu, S.R., Myat, A., Khambadkone, A., 2017. Energy optimization methodology of multi-chiller plant in commercial buildings. Energy 123, 64–76. https://doi.org/10.1016/j.energy.2017.01.116.
Vakiloroaya, V., Samali, B., Fakhar, A., Pishghadam, K., 2014. A review of different strategies for HVAC energy saving. Energy Convers. Manage. 77, 738–754. https://doi.org/10.1016/J.ENCONMAN.2013.10.023.
Wang, H., 2017. Empirical model for evaluating power consumption of centrifugal chillers. Energy Build 140, 359–370. https://doi.org/10.1016/J.ENBUILD.2017.02.019.
Wang, L., Lee, E.W., Yuen, R.K., 2018. A practical approach to chiller plants' optimisation. Energy Build 169, 332–343. https://doi.org/10.1016/j.enbuild.2018.03.076.
Wei, X., Xu, G., Kusiak, A., 2014. Modeling and optimization of a chiller plant. Energy 73, 898–907. https://doi.org/10.1016/J.ENERGY.2014.06.102.